Preparation and Adsorption Behavior of Aminated Electrospun Polyacrylonitrile Nanofiber Mats for Heavy Metal Ion Removal

ARTICLE *in* ACS APPLIED MATERIALS & INTERFACES · DECEMBER 2010

Impact Factor: 6.72 · DOI: 10.1021/am1008024 · Source: PubMed

Preparation and Adsorption Behavior of Aminated Electrospun Polyacrylonitrile Nanofiber Mats for Heavy Metal Ion Removal

Pimolpun Kampalanonwat and Pitt Supaphol*

The Petroleum and Petrochemical College and The Center for Petroleum, Petrochemicals and Advanced Materials, Chulalongkorn University, Phyathai Road, Pathumwan, Bangkok 10330, Thailand

ABSTRACT Polyacrylonitrile (PAN) nanofiber mats were prepared by electrospinning and they were further modified to contain amidino diethylenediamine chelating groups on their surface via heterogeneous reaction with diethylenetriamine (DETA). The obtained aminated PAN (APAN) nanofiber mats were evaluated for their chelating property with four types of metal ions, namely Cu(II), Ag(I), Fe(II), and Pb(II) ions. The amounts of the metal ions adsorbed onto the APAN nanofiber mats were influenced by the initial pH and the initial concentration of the metal ion solutions. Increasing the contact time also resulted in a monotonous increase in the adsorbed amounts of the metal ions, which finally reached equilibria at about 10 h for Cu(II) ions and about 5 h for Ag(I), Fe(II), and Pb(II) ions. The maximal adsorption capacities of the metal ions on the APAN nanofiber mats, as calculated from the Langmuir model, were 150.6, 155.5, 116.5, and 60.6 mg g^{-1}, respectively. Lastly, the spent APAN nanofiber mats could be facilely regenerated with a hydrochloric acid (HCl) aqueous solution.

KEYWORDS: electrospinning • aminated polyacrylonitrile • metal ion removal

1. INTRODUCTION

Nowadays, pollution of water from the contamination of heavy metals is a serious environmental problem. Metals such as chromium, copper, iron, lead, silver, and zinc, which have high toxic and nonbiodegradable properties, can cause problems to both the environment and the living organisms (1, 2). Many methods (such as adsorption, electroplating, ion exchange, membrane separation, precipitation, and so forth) are being used to remove the ions of these metals from aqueous effluents (3−7). Among these, adsorption is commonly regarded as an effective and economical method for wastewater treatment. Various types of adsorbents (such as activated carbons (8−10), chitosan/natural zeolites (11, 12), biosorbents (13−15), and chelating materials 16, 17)) have been studied for the adsorption of metal ions from aqueous solutions. The adsorption properties of these adsorbents depend on the functional group(s) on their surfaces, where it has been found that an adsorbent containing nitrogen-based ligands (such as, amino, amidoxime, imidazole, and hydrazine groups) was effective in forming complexation with metal ions (17−24).

Recently, nanoscopic materials are of great interests to be developed as efficient adsorbents for metal ions, because of their high surface area to unit mass ratios. There have been a number of research work on nanoadsorbents, which include nanobeads (25), nanocomposites (26), magnetic-nano adsorbents (27), and nanofibrous matrices (28). Among these materials, nanofibrous matrices have attracted a great deal of attention because of their many advantages, such as high porosity, high gas permeability, and high specific surface area per unit mass, which should lead to a high adsorption capacity. Polyacrylonitrile (PAN) microfibers, because of their availability as commodity textile materials, have been modified extensively to contain a chelating group for metal ion removal. Additionally, PAN can be easily prepared into nanoscopic fibrous materials by a facile fiber spinning process, namely electrospinning (29).

Electrospinning is a process capable of producing ultrafine fibers, with diameters in the nano- to micrometer range, from materials of diverse origins, including polymers (30). In the traditional setup, a polymer liquid (i.e., melt or solution) is first loaded into a container with a nozzle and then charged with a high electrical potential across a finite distance between the nozzle and a grounded collection device. When the electric field increases beyond a critical value, a charged stream of the polymer liquid (i.e., charged jet) is ejected (31). As the jet travels to the collector, it either cools down (for the melt) or the solvent evaporates (for the solution) to finally obtain ultrafine fibers in the form of a nonwoven fabric on the collector. The morphology of the electrospun fibers is influenced by a number of factors, such as solution properties, processing conditions, and ambient conditions (32). The proposed uses for these fibers are, for examples, as scaffolding materials for tissue engineering (33) and carriers for the delivery of DNA and drugs (34, 35). Furthermore, the introduction of appropriate functional groups on the surface of an electrospun nanofiber mat enables its utilization as an adsorbent in wastewater treatment (28). It is therefore of our interest to investigate the

* Corresponding author. Tel.: +66 2218 4131. Fax: +66 2215 4459. E-mail: pitt.s@chula.ac.th.

Received for review August 29, 2010 and accepted November 11, 2010

DOI: 10.1021/am1008024

feasibility of using a nanofiber mat that bears amine groups on its surface as an adsorbing substrate of metal ions.

The purpose of the present contribution was to synthesize aminated PAN (APAN) nanofiber mats from the reaction between electrospun PAN nanofiber mats and diethylenetriamine (DETA). Characterization of the obtained nanofiber mats was studied by Fourier-transform infrared spectroscopy (FT-IR) and scanning electron microscopy (SEM). The effects of the pH, the contact time, and the initial metal ion concentration on the adsorption capacity of the APAN nanofiber mats for Cu(II), Ag(I), Fe(II), and Pb(II) ions were examined by atomic absorption spectroscopy (AAS). Desorption of the metal ions from the preadsorbed APAN nanofiber mats was also examined using hydrochloric acid (HCl) aqueous solutions of varying concentrations.

2. EXPERIMENTAL SECTION

2.1. Materials. Polyacrylonitrile (PAN) microfibers, used as the raw material for preparing the base PAN solution which was later fabricated into ultrafine PAN fiber mats by electrospinning, were received from Thai Acrylic Fiber Co., Ltd. (Thailand). The polymer ($M_w \approx 55.5$ kDa) contained 91.4 wt % acrylonitrile monomer (CH_2═$CHCN$) and 8.6 wt. % methylacrylate comonomer (CH_2═$CHCOOHCH_3$). Dimethylformamide (DMF; ~99.98 % purity) and ethanol (analytical reagent grade) were purchased from Lab-scan Asia Co., Ltd. (Thailand). Diethylenetriamine (DETA; ~99 % purity) and aluminum chloride hexahydrate ($AlCl_3 \cdot 6H_2O$; ~99 % purity) were purchased from Sigma-Aldrich (USA). Stock solutions of metal ions were prepared from copper(II) chloride dihydrate ($CuCl_2 \cdot 2H_2O$, ~99 % purity; Sigma-Aldrich, USA), silver nitrate ($AgNO_3$, ~99.998 % purity; Fisher Scientific, USA), lead(II) nitrate [$Pb(NO_3)_2$, ~99 % purity; Ajax Finechem, Australia], and iron(II) sulfate ($FeSO_4$, ~99 % purity; Ajax Finechem, Australia).

2.2. Electrospun Fibers from PAN Solution. Electrospun PAN fiber mats were prepared in a similar manner to that reported by Sutasinpromprae et al. (29). Briefly, the base PAN solution was prepared at 10 wt % from the as-received PAN microfibers in DMF. The as-prepared solution was then electrospun under a fixed electric field of 15 kV/20 cm, using a Gamma High Voltage Research D-ES30PN/M692 dc power supply, onto an aluminum (Al) sheet wrapped around a rotating cylinder (width and OD of the cylinder ≈ 15 cm; rotational speed ≈ 50 rpm), which was used as the collector. Each of the electrospun fiber mats was collected continuously for 48 h (resulting in the fiber mats of 125 ± 10 μm in thickness). Prior to further uses, these PAN fiber mats were placed in vacuo at room temperature (25 ± 1 °C) to remove as much solvent from them as possible.

2.3. Preparation of Aminated PAN Nanofiber Mats. Aminated PAN (hereafter, APAN) nanofiber mats were synthesized based on a procedure that was adapted from the work of Ko et al. (24). Briefly, about 0.6 g of the electrospun PAN fiber mats was placed into a sealed chamber containing 50 mL of DETA and 2.0 g of $AlCl_3 \cdot 6H_2O$. The reaction temperature was fixed at 90 °C and the reaction time was varied from 1 to 5 h. After the reaction, the obtained fiber mats were washed successively with distilled water and ethanol, and were then dried in vacuo at room temperature (25 ± 1 °C). For comparative purposes, APAN fibers were also synthesized from the as-received PAN microfibers at 90 °C with the reaction time being selected from the optimal condition used in the preparation of the APAN nanofiber mats.

2.4. Characterization. Morphologies of both of the PAN and the APAN nanofiber mats were observed by a JEOL JSM-6400 scanning electron microscope (SEM). Each specimen was coated with a thin layer of gold using a JEOL JFC-1100E sputtering device prior to the SEM observation. The diameters of no less than 50 individual fiber segments for a given fiber mat specimen were measured from the SEM images using SemAphore 4.0 software, from which the average and the standard deviation values were calculated. A Thermo-Nicolet Nexus 670 Fourier-transform infrared spectroscope (FT-IR), operating at a resolution of 4 cm^{-1} and a wavenumber range of 4000 to 400 cm^{-1}, was used to characterize the neat and the modified electrospun PAN fiber mats, based on the KBr method. The conversion of the nitrile group into the amidino diethylenediamine group (C_n, in %) on the surface of each of the modified PAN fiber mats was estimated based on the following equation (28)

$$C_n = \frac{W_1 - W_0}{W_0}\frac{M_0}{M_1}100 \quad (1)$$

where W_1 and W_0 are the weights of the PAN fiber mat after and before the reaction (i.e., 0.6 g), M_0 is the molecular weight of the acrylonitrile monomer (i.e., 53 g mol^{-1}) and M_1 is the molecular weight of DETA (i.e., 103 g mol^{-1}). The weights of the samples after the reaction were measured using a Sartorius BS 224S digital balance, which has a measurement resolution of 0.1 mg.

2.5. Adsorption Behavior. 2.5.1. *Effects of pH and Contact Time.* The APAN nanofiber mat specimens (i.e., 0.1 g each) were individually placed in a flask containing 20.0 mL solution of Cu(II), Ag(I), Pb(II), or Fe(II) ions. The initial concentration of the ions was 200 ppm. Each flask was shaken in a thermostatic shaker bath, operating at 30 °C and 100 rpm. To investigate the effect of pH, we adjusted the initial pH of the testing solutions between 2.0 and 7.0, using either 0.1 M HCl or 0.1 M NaOH aqueous solution. To refrain the metal ions from precipitation, the pH of greater than 7.0 was not studied. To investigate the effect of contact time, the initial pH of the testing solutions was chosen from the optimal pH value that resulted in high adsorption of the metal ions. In either case, 1 mL of each of the testing solutions was withdrawn (at 24 h, in case of the effect of pH, and at an arbitrary time point, ranging from 0 to 24 h, in case of the effect of contact time) and diluted with a proper amount of distilled water (i.e., sample solution). The sample solutions were then quantified for the amounts of metal ions by a Varian SpectrAA-300 atomic absorption spectroscope (AAS).

The amount of the metal ions adsorbed onto each fiber mat specimen (i.e., the adsorption capacity (q, in mg g^{-1})) was calculated on the basis of the following equation (28)

$$q = \frac{(C_0 - C_e)V}{M} \quad (2)$$

where C_0 and C_e are the initial and the equilibrium concentrations of the metal ions in the testing solution (mg L^{-1}), V is the volume of the testing solution (L), and M is the weight of the adsorbent (i.e., 0.1 g).

2.5.2. *Adsorption Isotherms.* The adsorption isotherm of each type of the metal ions on the APAN nanofiber mats was studied by placing nanofiber mat specimens (0.1 g each) in a series of flasks containing 20.0 mL solutions of Cu(II), Ag(I), Pb(II), or Fe(II) ions of varying initial concentrations, ranging from 40 to 1000 ppm. The initial pH of the testing solutions was the same as that used in the experiment for studying the effect of the contact time. The flasks were each equilibrated in the shaker bath, operating at 30 °C and 100 rpm. After the 24 h contacting period, 1 mL of each of the testing solutions was

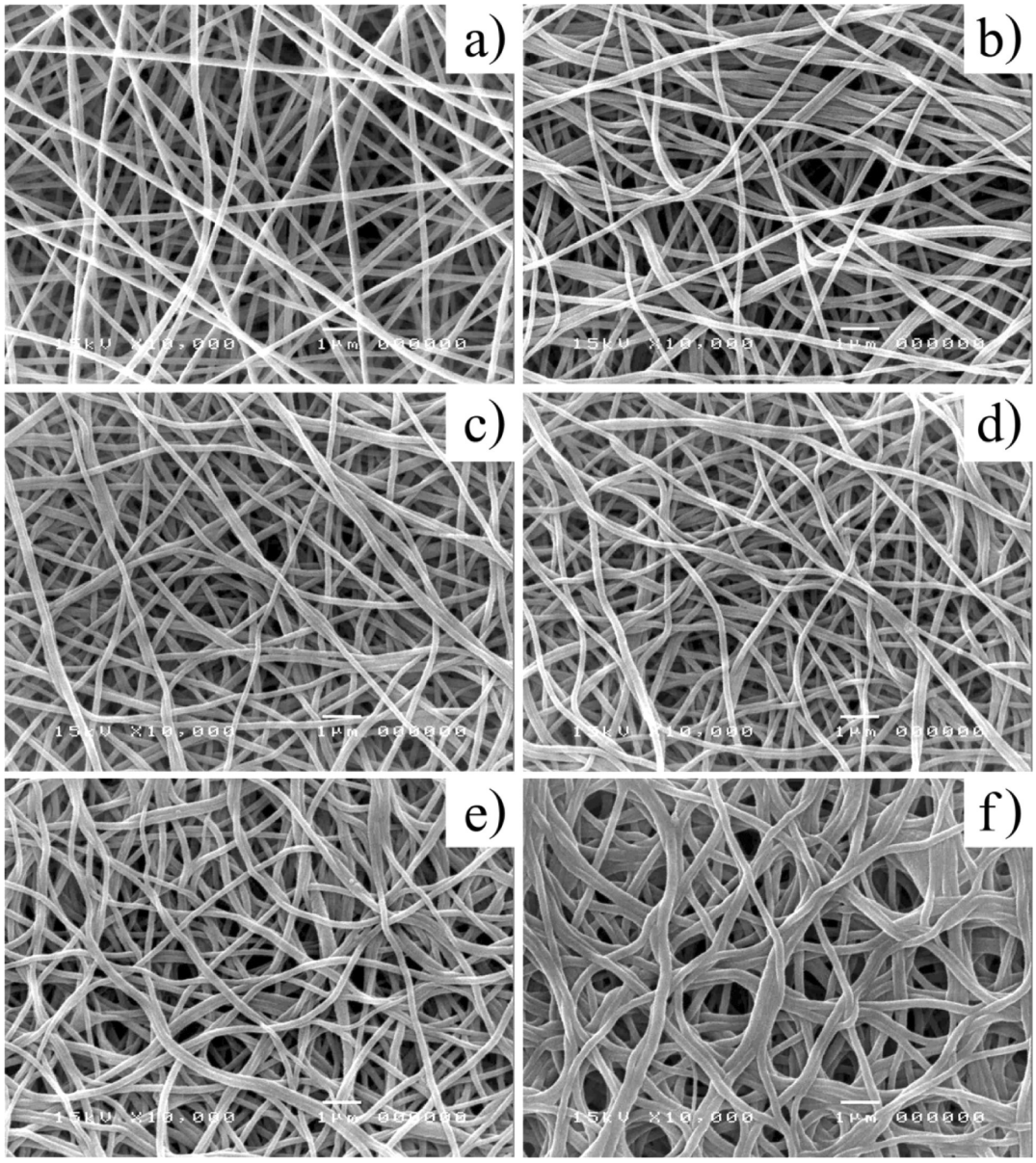

FIGURE 1. Representative SEM images of (a) the neat electrospun PAN fiber mat and the APAN electrospun fiber mats that had been obtained from the reaction between the neat PAN electrospun fiber mat and DETA in the presence of $AlCl_3 \cdot 6H_2O$ at 90 °C for (b) 1, (c) 2, (d) 3, (e) 4, and (f) 5 h.

withdrawn, diluted with a proper amount of distilled water, and quantified for the amount of metal ions by AAS. Equation 2 was used to calculate the adsorption capacities of the obtained data.

2.6. Desorption Behavior. The APAN fiber mat specimens (0.1 g each), that had been preadsorbed with the metal ions according to the procedure set-forth in section 2.5.1 for 24 h at the optimal initial pH condition for each metal ion solution (initial concentration = 200 ppm), were used in the desorption studies. The preadsorbed amounts of the ions were determined by AAS to be 3.93 ± 0.06 mg for Cu(II) ions, 3.90 ± 0.07 mg for Ag(I) ions, 3.91 ± 0.08 mg for Fe(II) ions, and 3.92 ± 0.03 mg for Pb(II) ions. After the preadsorption procedure, the fiber mat specimens were rinsed with distilled water to remove any residual solution and were then dried in vacuo at room temperature (25 ± 1 °C). The desorption of metal ions was carried out in 20 mL of HCl aqueous solutions of varying concentrations, ranging from 2 to 10 M. The contents of the flasks were shaken at 100 rpm and 30 °C for 1 h. The ion concentrations in the solutions were analyzed by AAS. The desorption ratio (D, in %), for each data point, was calculated based on the percentage of the ratio between the desorbed and the initial, preadsorbed amounts of the ions.

3. RESULTS AND DISCUSSION

3.1. Characterization of APAN Nanofiber Mats. Morphologies of the neat and the aminated PAN nanofiber mats were observed by SEM and the results are shown in Figure 1. Evidently, the cross sections of the neat PAN fibers were round and their surfaces were smooth. The diameters of these fibers were rather uniform, with the values being 192 ± 55 nm. The size of these fibers was comparable to that reported by Sutasinpromprae et al. (29). Reacting the neat PAN fibers with DETA for 1 h caused the obtained APAN fibers to be more intertwined without expressing a strong influence on their overall morphology, as the cross-sections of the majority of the fibers were still round and their surfaces were still smooth. Nevertheless, there was evidence

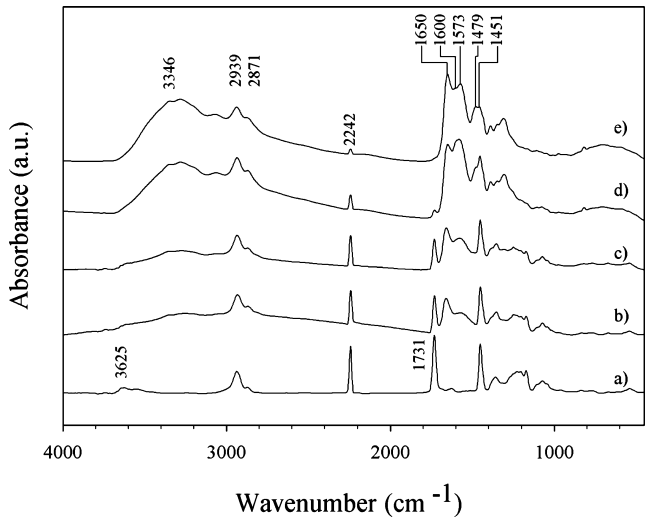

FIGURE 2. FT-IR spectra of (a) the neat electrospun PAN fiber mat and the APAN electrospun fiber mats that had been obtained from the reaction between the neat PAN electrospun fiber mat and DETA in the presence of $AlCl_3 \cdot 6H_2O$ at 90 °C for (b) 1, (c) 2, (d) 3, and (e) 4 h.

of adjacent fiber segments conglutinating to each other at touching points. Increasing the reaction time up to 4 h only caused the obtained APAN fibers to become more intertwined and the occurrence of fiber segments conglutinating to each other at touching points was more frequent. The diameters of the APAN electrospun fibers that had been reacted for 1, 2, 3, and 4 h were 194 ± 50, 198 ± 60, 186 ± 60, and 196 ± 60 nm, respectively. Clearly, the size of the obtained fibers was essentially similar to that of the neat PAN fibers. For the PAN nanofiber mats that had been reacted for 5 h, the conglutination of adjacent fibers was so severe that the materials started to lose their individually fibrous character. Moreover, the size of these fibers increased sharply to 231 ± 75 nm. Because of the considerable change to the morphology of the obtained APAN electrospun fibers, the reaction time of 5 h was not considered further. Since 4 h was the longest reaction time that did not result in the noticeable change in the morphology of the fibers, it was chosen to prepare the APAN nanofiber mat for further studies.

The FT-IR spectra of the neat and the aminated PAN nanofiber mats are shown in Figure 2. The spectrum of the neat PAN fiber mat exhibited adsorption peaks at 2242 and 1731 cm^{-1}, corresponding to the stretching vibrations of the nitrile group and the carbonyl group of the ester of the methylacrylate comonomer (28), respectively. The spectra of the APAN fiber mats, on the other hand, showed new absorption bands at 3346, 1650, 1600, 1573, and 1479 cm^{-1}. These can be assigned to the stretching vibrations of the secondary amine (N−H), the amidine group (N−C═N) and the primary amine (NH_2), and the bending vibrations of the secondary amine and the methyl group of DETA, respectively (22, 24). The intensities of these peaks increased with an increase in the reaction time. The reduction of the carbonyl ester peak with an increase in the reaction time, hence the conversion, indicates the disappearance of the methylacrylate group from the surface of the PAN nanofibers upon reacting with DETA (22, 24). The peak associated with the nitrile group of the APAN nanofiber mats at 2242 cm^{-1} also decreased in its intensity as the conversion increased (Table 1). Moreover, the reason for the conversion value of the APAN nanofiber mat which was greater than that of the corresponding APAN microfibers (Table 1) should be a direct result of the specific surface area of the electrospun PAN fiber mat that was greater than that of the PAN microfibers. Based on the FT-IR results, the mechanism of the reaction between PAN and DETA could be proposed as Scheme 1.

3.2. Adsorption Behavior. ***3.2.1. Effect of pH.*** The adsorption of metal ions on the surface of the APAN nanofiber mats that had been prepared at the reaction time of 4 h was studied and the results are shown as a function of the initial pH of the testing solutions in Figure 3. At the lowest initial pH investigated, small amounts of metal ions could be adsorbed onto the materials, due particularly to the competitive adsorption between the prevalently available H^+ and the metal ions. Moreover, the positive charges as resulting from the protonation of the primary and the secondary amines of the DETA ligands gave a strong electrostatic repulsive force to the positively charged metal ions (27). The amounts of the metal ions adsorbed onto the APAN nanofibers increased significantly with an increase in the initial pH of the testing solutions. As the amounts of the protons decreased, the number of the protonated amine groups also decreased. As a result, more amine groups are available to capture the metal ions (i.e., via the interaction

Table 1. Conversion (C_n, in %) of the Nitrile Group of the Neat Electrospun PAN Nanofibers and the As-Received PAN Microfibers into the Amidino Diethylenediamine Group of the Corresponding APAN Fibers at Different Reaction Times ($n = 5$)

	electrospun PAN nanofibers				as-received PAN microfibers
reaction time (h)	1	2	3	4	4
% conversion	13.4 ± 1.3	18.3 ± 1.3	45.7 ± 1.42	58.5 ± 2.4	31.6 ± 2.9

Scheme 1. Chemical Reaction between PAN and DETA

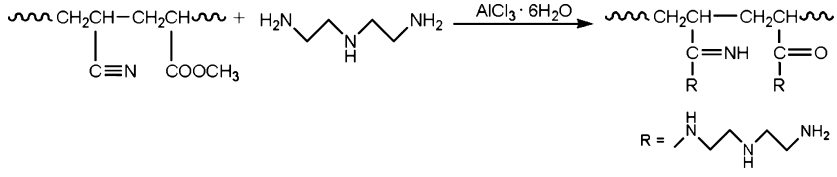

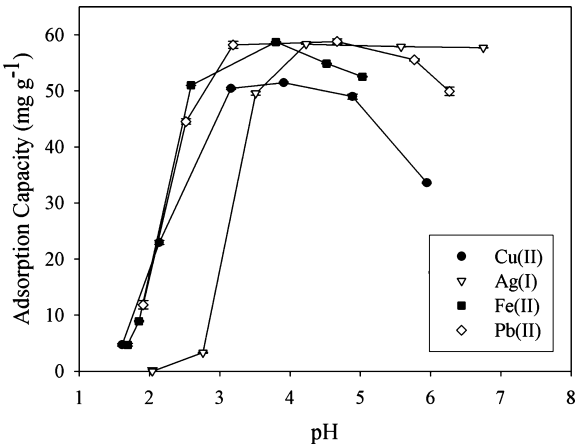

FIGURE 3. Effect of the initial pH of the testing solutions on the adsorption of Cu(II), Ag(I), Fe(II), and Pb(II) ions onto the APAN nanofiber mats ($n = 5$). Experimental conditions: initial ion concentration = 200 ppm, sample dose = 0.1 g/20 mL, temperature = 30 °C, and contact time = 24 h.

of the metal ions with the lone-pair electrons of nitrogen) (13). Further increase in the initial pH of the testing solutions resulted in the amounts of the adsorbed metal ions reaching plateau values, and in most cases (except for the adsorption of Ag(I) ions), the amounts of the adsorbed metal ions decreased as the initial pH approached the neutrality (25, 37−39). This could be due to the competitive adsorption from the OH^- ions via the formation of the hydrogen bonding, resulting in the reduction of the adsorptive sites on the surface of the APAN nanofibers. Moreover, at these pH levels, the concentration of OH^- ions is high enough to interact with the metal ions, reducing the availability of the metal ions in their free, hydrated form to interact with the amine groups of the DETA ligands.

At the initial concentration of the metal ions in the testing solutions of 200 ppm, the optimal, initial pH level was found to be 4.0, as 90.5, 99.9, 100, and 97.0% of Cu(II), Ag(I), Fe(II), and Pb(II) ions could be removed from the testing solutions. Consequently, the initial pH of 4.0 was chosen for subsequent studies.

3.2.2. Effect of Contact Time. Figure 4 shows the effect of the contact time on the adsorption capacity of the APAN nanofiber mats, the APAN microfibers, and the as-received PAN microfibers for Cu(II), Ag(I), Fe(II), and Pb(II) ions. The adsorption of all of the four metal ions on the PAN microfibers was low, with the maximal values being at about 20%. This should be a result of the weak interaction between the metal ions and the lone-pair nitrogen electrons of the nitrile group on the surface of the fibers (25). For the APAN nanofiber mats and the APAN microfibers, considerably greater amounts of metal ions could be adsorbed on these materials, a direct result of the introduction of the acryloamidino diethylenediamine group on their surfaces (21−24, 27). Clearly, the adsorption increased with an increase in the contact time and reached equilibria within 10 h for the Cu(II) ions and 5 h for the Ag(I), Fe(II), and Pb(II) ions. There are two steps in the adsorption of these metal ions. In the initial step, adsorption was swift because of the great number of free adsorptive sites and the high concentration of the metal ions. In the second step, adsorption rates decreased and finally reached equilibria. This was the direct effect from the depletion of the adsorptive sites as well as the decrease in the metal ion concentration in the testing solutions (10). Comparatively, preferential adsorption of Cu(II) ions was observed on the APAN nanofiber mats, whereas both types of substrates exhibited similar adsorption toward the rest of the metal ions investigated. To ensure the equilibratory adsorption of the metal ions on the APAN nanofiber mats, we chose the contact time of 24 h for subsequent studies.

3.2.3. Adsorption Isotherms. The effect of the initial concentration (C_0) of the metal ions in the testing solutions on the adsorption capacities of the APAN nanofiber mats toward the four metal ions is shown in Figure 5. The results are reported as the functions of the equilibrium adsorption capacities of the metal ions (q_e) versus the equilibrium concentration of the ions in the testing solutions (C_e). For most types of the tested metal ions (in exception to Cu(II) ions), q_e increased sharply with an initial increase in C_e (whereas that for Cu(II) ions increased rather gradually) and reached a saturation point as C_e increased further. Various mathematical models can be used to analyze adsorption data. The most common ones are the Langmuir and the Freundlich models (13, 40).

The Langmuir model was derived to describe the adsorption of an adsorbate on a homogeneous, flat surface of an adsorbent and each adsorptive site can be occupied only once in a one-on-one manner. Mathematically, the model can be written as follows (27, 28)

$$\frac{C_e}{q_e} = \frac{C_e}{q_m} + \frac{1}{K_L q_m} \tag{3}$$

where q_m denotes the maximal adsorption capacities of the metal ions on the adsorbent ($mg \cdot g^{-1}$) and K_L is the adsorption equilibrium constant ($L\ mg^{-1}$). The value of q_m is taken as the inverse value of the slope of the plot of C_e/q_e versus C_e, whereas that of K_L can be calculated from the values of the slope and the y-intercept of the plot (i.e., slope/y-intercept). The values of these parameters, as analyzed from the plots shown in Figure 5, are summarized in Table 2.

Unlike the Langmuir model, the Freundlich model is used to describe the adsorption of an absorbate on a heterogeneous surface of an adsorbent. The mathematical expression of the model is given as follows (27)

$$q_e = K_F C_e^{1/n} \tag{4}$$

where K_F ($mg^{(1-1/n)}\ L^{1/n}\ g^{-1}$) and n are Freundlich constants. By plotting log q_e as a function of log C_e, the value of K_F is taken as the antilogarithmic value of the y-intercept and n is the inverse value of the slope. The values of these parameters, which were also analyzed from the plots shown in Figure 5, are summarized in Table 2.

According to the obtained results, the adsorption data of the four metal ions on the APAN nanofiber mats were fitted

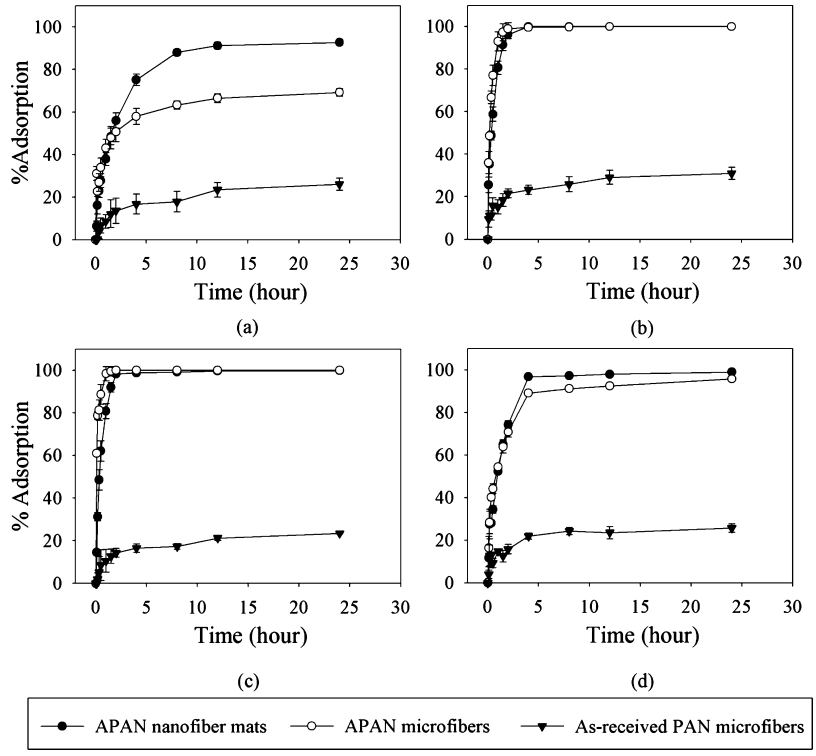

FIGURE 4. Effect of contact time on the adsorption of (a) Cu(II), (b) Ag(I), (c) Fe(II), and (d) Pb(II) ions onto the APAN nanofiber mats, the APAN microfibers, and the as-received PAN microfibers ($n = 5$). Experimental conditions: initial ion concentration = 200 ppm, sample dose = 0.1 g/20 mL, initial pH 4.0, and temperature = 30 °C.

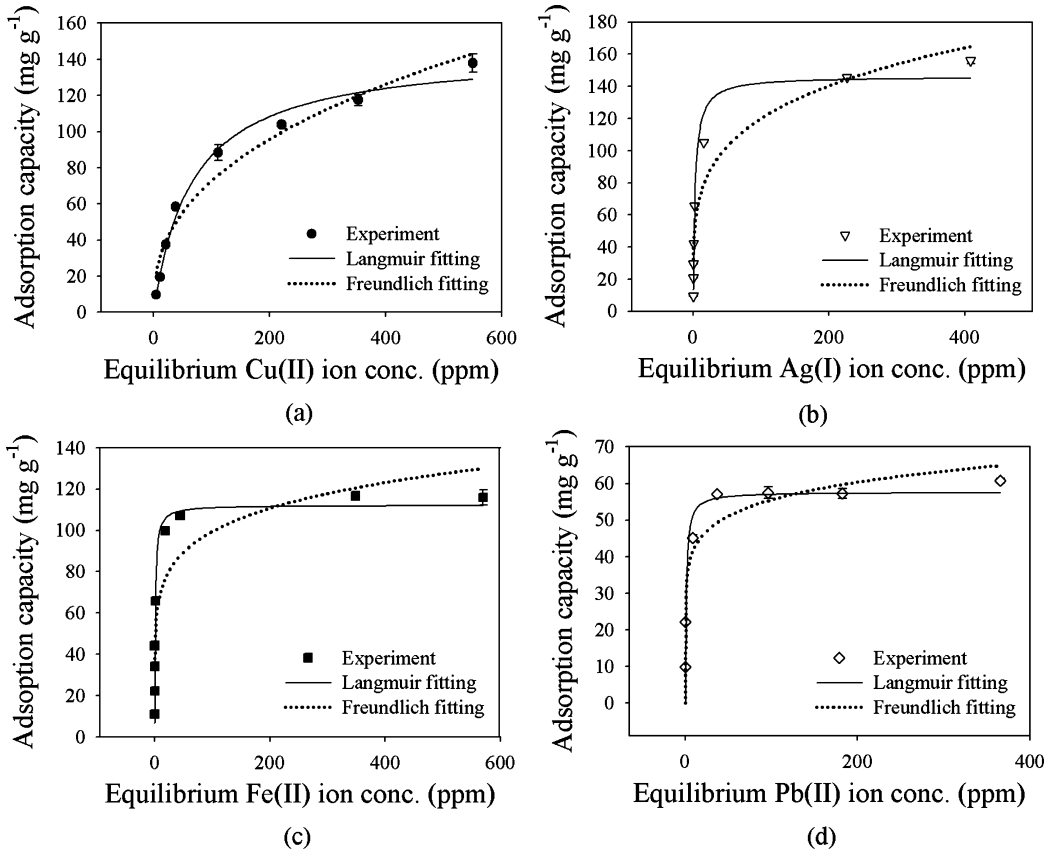

FIGURE 5. Adsorption isotherms of Cu(II), Ag(I), Fe(II), and Pb(II) ions onto the APAN nanofiber mats ($n = 5$). Experimental conditions: initial ion concentration = 40−1000 ppm, sample dose = 0.1 g/20 mL, initial pH 4, temperature = 30 °C, and contact time = 24 h.

particularly well with the Langmuir model, as indicated by the very high values of the correlation coefficient (r^2). As shown in Table 2, the maximal adsorption capacities of Cu(II), Ag(I), Fe(II), and Pb(II) ions on the APAN nanofiber

Table 2. Values of the Parameters Associated with the Langmuir and Freundlich Models, Including Those of the Correlation Coefficient, for the Adsorption of Cu(II), Ag(I), Fe(II), and Pb(II) Ions on the APAN Nanofiber Mats and the Corresponding APAN Microfibers

		Langmuir model			Freundlich model		
adsorbent	metal ions	q_m (mg g^{-1})	K_L (L mg^{-1})	r^2	K_F (mg$^{(1-1/n)}$ L$^{1/n}$ g^{-1})	n	r^2
APAN nanofiber mat	Cu(II)	150.6	0.013	0.9923	13.43	2.66	0.9644
	Ag(I)	155.5	0.216	0.9989	50.82	5.03	0.9379
	Fe(II)	116.5	0.613	0.9999	31.92	2.80	0.9813
	Pb(II)	60.6	0.342	1.0000	22.13	3.43	0.9663
APAN microfiber	Cu(II)	66.6	0.024	0.9947	6.9	2.66	0.9888
	Ag(I)	105.7	0.804	0.9999	33.9	3.22	0.7975
	Fe(II)	75.0	0.058	0.9989	11.8	3.01	0.7749
	Pb(II)	28.4	0.137	0.9998	9.2	4.97	0.8009

mats were 150.6, 155.5, 116.5, and 60.6 mg g^{-1}, respectively. These values were greater than those of the APAN microfibers that had been prepared at the same condition used to obtain the APAN nanofiber mats (see Table 2). This should be a direct result of the much greater specific surface area for adsorption of the APAN nanofiber mats. In the section 3.2.2, however, it was shown that both of the APAN nanofiber mats and the APAN microfibers exhibited similar adsorption toward almost all of the metal ions, except for Cu(II) ions. This was due to the fact that the initial concentration of the metal ion solutions in that particular study was rather low (i.e., 200 ppm). At such a low initial concentration of the metal ions, almost all of the metal ions in the solution could readily be adsorbed on both types of the substrates.

3.3. Adsorption Kinetics. The results as obtained in the section 3.2.2 were further analyzed to obtain the information on the adsorption kinetics of the four metal ions on the APAN nanofiber mats. The pseudo-first-order kinetic model is based on the approximation that the adsorption rate relates to the number of the unoccupied, adsorptive sites. The model, in its final form, can be written as follows (36, 41)

$$\log(q_e - q_t) = \log q_e - \frac{k_1}{2.303}t \qquad (5)$$

where q_t is the adsorption capacity of the metal ions on an adsorbent at an arbitrary time t (mg g^{-1}) and k_1 is the pseudofirst-order rate constant (min^{-1}). By plotting $\log(q_e - q_t)$ as a function of the contact time t, the values of the calculated q_e (i.e., $q_{e,cal}$) and the rate constant k_1 can be obtained from the antilogarithmic value of the y-intercept and the slope of the plot, respectively. The adsorption of Cu(II), Ag(I), Fe(II), and Pb(II) ions onto the APAN nanofiber mats at the initial concentration of 200 ppm, as shown in Figure 4, were analyzed. The results are graphically shown in Figure 6, whereas the values of k_1 and $q_{e,cal}$ along with those of the correlation coefficient (r^2) are summarized in Table 3.

On the other hand, the adsorption rate could also be approximated on the basis of the pseudo-second-order kinetic model. This model is derived based on the notion that the adsorption should relate to the squared product of the difference between the number of the equilibrium adsorptive sites available on an adsorbent and that of the occupied sites. The model, in its final form, can be expressed as follows (36, 41)

$$\frac{t}{q_t} = \frac{1}{k_2 q_e^2} + \frac{t}{q_e} \qquad (6)$$

where k_2 is the pseudosecond-order rate constant (g mg^{-1} min^{-1}). The analyses of the data, such as those shown in Figure 4, could be done through the construction of plots of t/q_t as a function of the contact time t, as shown in Figure 7. Linear plots should be obtained, with the values of the calculated q_e (i.e., $q_{e,cal}$) and the rate constant k_2 can be obtained from the inverse values of the slope and the y-interception values, respectively. The values of k_2 and $q_{e,cal}$ along with those of the correlation coefficient (r^2) are also summarized in Table 3.

On the basis of the values of the correlation coefficient (r^2), we fitted the experimental data better with the pseudo-second-order kinetic model than the pseudo-first-order kinetic model. Moreover, the $q_{e,cal}$ values as obtained from the pseudo-second -order kinetic model appeared to be very close to the experimentally observed values than do the values from the pseudo-first-order kinetic model.

3.4. Desorption Characteristics. The desorption behavior of the APAN nanofiber mats that had been pread-

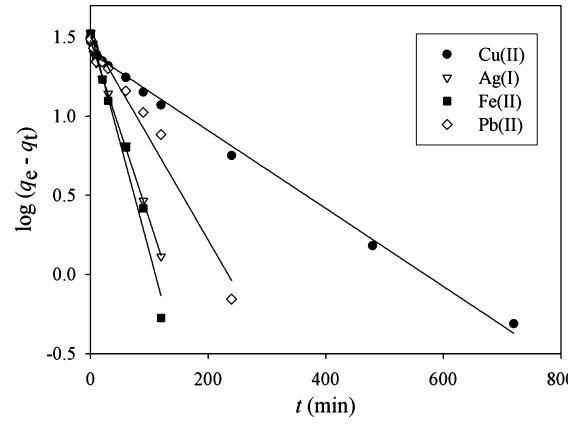

FIGURE 6. Adsorption kinetics of Cu(II), Ag(I), Fe(II), and Pb(II) ions onto the APAN nanofiber mats (see results in Figure 4), based on the pseudo-first-order kinetic model.

Table 3. Kinetics Parameters Describing the Adsorption of Cu(II), Ag(I), Fe(II), and Pb(II) Ions onto the APAN Nanofiber Mats (see results in Figure 4) Based on the Pseudo-First- and the Pseudo-Second-Order Kinetic Models

		pseudo first order			pseudo second order		
metal ions	$q_{e,exp}$ (mg g^{-1})	k_1 (min^{-1})	$q_{e,cal}$ (mg g^{-1})	r^2	k_2 (min^{-1})	$q_{e,cal}$ (mg g^{-1})	r^2
Cu(II)	29.62	5.67×10^{-3}	25.23	0.9944	4.29×10^{-4}	31.40	0.9987
Ag(I)	33.51	2.60×10^{-2}	29.99	0.9975	2.18×10^{-3}	33.97	0.9998
Fe(II)	33.20	3.20×10^{-2}	34.04	0.9809	1.90×10^{-3}	33.70	0.9997
Pb(II)	30.58	1.48×10^{-2}	31.62	0.9704	7.46×10^{-4}	31.72	0.9989

sorbed with the metal ions upon their submersion in 20 mL of 2−10 M HCl aqueous solutions for 1 h is graphically shown in Figure 8. For a given type of the metal ions, increasing the HCl concentration resulted in a monotonous increase in the desorbed amounts of the ions. Based on the obtained results, the desorption efficiency of over 90% could be achieved with the use of 10 M HCl solution as the desorbing solution. Though not shown, increasing the submersion time in the HCl solution also resulted in a monotonous increase in the desorbed amounts of the ions.

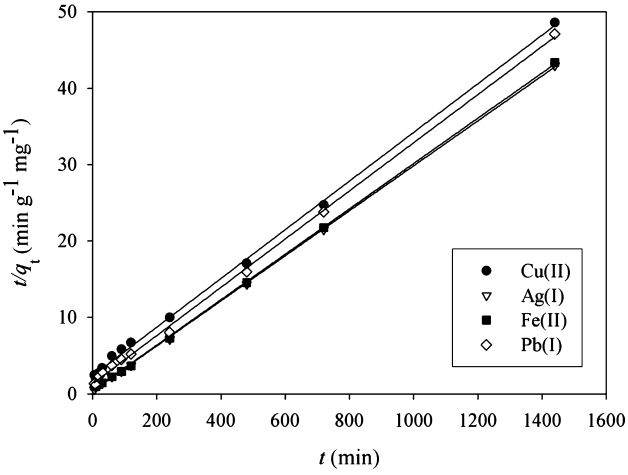

FIGURE 7. Adsorption kinetics of Cu(II), Ag(I), Fe(II), and Pb(II) ions onto the APAN nanofiber mats (see results in Figure 4), based on the pseudo-second-order kinetic model.

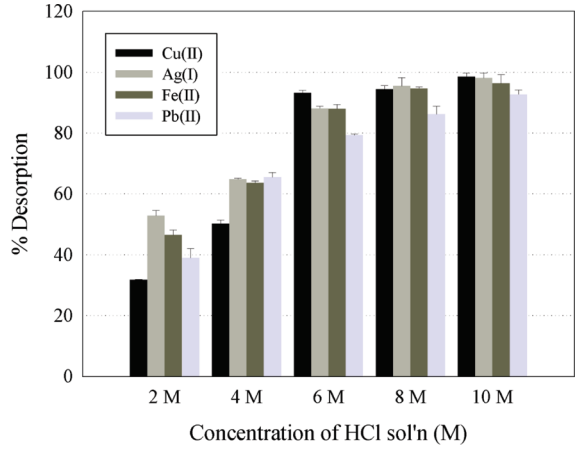

FIGURE 8. Desorption of Cu(II), Ag(I), Fe(II), and Pb(II) ions from the APAN nanofiber mats that had been preadsorbed with the metal ions (initial ion concentration = 200 ppm, initial pH 4.0, sample dose = 0.1 g/20 mL, temperature = 30 °C, and contact time = 24 h) as a function of submersion time in 20 mL of HCL aqueous solutions of varying concentrations for 1 h at 30 °C.

4. CONCLUSIONS

The APAN nanofiber mats were obtained from the reaction between the electrospun PAN nanofiber mats and DETA. The conversion of the nitrile group, native to PAN, into the amidino diethylenediamine group, native to APAN, increased with an increase in the reaction time. The chelating property of the obtained APAN nanofiber mats was evaluated against Cu(II), Ag(I), Fe(II), and Pb(II) ions. The initial pH of the testing solutions posed a strong influence on the adsorption behavior of the materials, with the initial pH of 4.0 being the optimal value where the APAN nanofiber mats showed high adsorption toward all four types of the metal ions. On the other hand, the adsorption capacity was found to increase with an increase in the contact time and the equilibria were reach at about 10 h for Cu(II) ions and about 5 h for the rest. The adsorption of these metal ions was fitted well with the Langmuir equation, with the maximal adsorption capacities being 150.6, 155.5, 116.5, and 60.6 mg g^{-1} for Cu(II), Ag(I), Fe(II), and Pb(II) ions, respectively. The transient adsorption data of the four metal ions on the APAN nanofiber mats were better described with the pseudo-second-order kinetic model. Lastly, submersion of the spent APAN nanofiber mats in 20 mL of 10 M HCl aqueous solution resulted in the desorption of more than 90% of the adsorbed amounts of the tested metal ions. The obtained results suggested that the APAN nanofiber mats possess a tremendous potential for use as a heterogeneous adsorbent for metal ions in wastewater effluents.

Acknowledgment. The authors acknowledge the partial support received from The Petroleum and Petrochemical College (P.P.C., Chulalongkorn University) and the doctoral scholarship received from the Royal Golden Jubilee PhD Program, The Thailand Research Fund (T.R.F.) (PHD/0164/2550).

REFERENCES AND NOTES

(1) Mahmoud, M. E.; Osman, M. M.; Hafez, O. F.; Elmelegy, E. *J. Hazard. Mater.* **2010**, *173*, 349–357.
(2) Shukla, S. R.; Pai, R. S.; Shendarkar, A. D. *Sep. Purif. Technol.* **2006**, *47*, 141–147.
(3) Navarro, R. R.; Wada, S.; Tatsumi, K. *J. Hazard. Mater. B* **2005**, *123*, 203–209.
(4) Panayotova, T.; Dimova-Todorova, M.; Dobrevsky, I. *Desalination* **2007**, *206*, 135–140.
(5) Dąbrowski, A.; Hubicki, Z.; Podkościelny, P.; Robens, E. *Chemosphere* **2004**, *56*, 91–106.
(6) Mbareck, C.; Nguyen, Q. T.; Alaoui, O. T.; Barillier, D. *J. Hazard. Mater.* **2009**, *171*, 93–101.
(7) O'Connell, D. W.; Birkinshaw, C.; O'Dwyer, T. F. *Bioresour. Technol.* **2008**, *99*, 6709–6724.

(8) Zhu, S.; Yang, N.; Zhang, D. *Mater. Chem. Phys.* **2009**, *113*, 784–789.
(9) Zhang, S.; Li, X.; Chen, J. P. *Carbon* **2010**, *48*, 60–67.
(10) Mishra, P. C.; Patel, R. K. *J. Hazard. Mater.* **2010**, *168*, 319–325.
(11) Dragan, E. S.; Dinu, M. V.; Timpu, D. *Bioresour. Technol.* **2010**, *101*, 812–817.
(12) Wang, X.; Zheng, Y.; Wang, A. *J. Hazard. Mater.* **2009**, *168*, 970–977.
(13) Shen, W.; Chen, S.; Shi, S.; Li, X.; Zhang, X.; Hu, W.; Wang, H. *Carbohyd. Polym.* **2009**, *75*, 110–114.
(14) Jiang, Y.; Pang, H.; Liao, B. *J. Hazard. Mater.* **2009**, *164*, 1–9.
(15) Zhang, G.; Qu, R.; Sun, C.; Ji, C.; Chen, H.; Wang, C.; Niu, Y. *J. Appl. Polym. Sci.* **2008**, *110*, 2321–2327.
(16) Sun, S.; Wang, A. *Sep. Purif. Technol.* **2006**, *51*, 409–415.
(17) Kavaklı, P. A.; Güven, O. *J. Appl. Polym. Sci.* **2004**, *93*, 1705–1710.
(18) Bilba, N.; Bilba, D.; Moroi, G. *J. Appl. Polym. Sci.* **2004**, *92*, 3730–3735.
(19) Gong, B. *Talanta* **2002**, *57*, 89–95.
(20) Chang, X.; Su, Q.; Liang, D.; Wei, X.; Wang, B. *Talanta* **2002**, *57*, 253–261.
(21) Deng, S.; Bai, R. *Water Res.* **2004**, *38*, 2424–2432.
(22) Deng, S.; Bai, R.; Chen, J. P. *Langmuir* **2003**, *19*, 5058–5064.
(23) Ma, N.; Yang, Y.; Chen, S.; Zhang, Q. *J. Hazard. Mater.* **2009**, *171*, 288–293.
(24) Ko, Y. G.; Choi, U. S.; Park, Y. S.; Woo, J. W. *J. Polym. Sci., Polym. Chem.* **2004**, *42*, 2010–2018.
(25) Türkmen, D.; Yılmaz, E.; Öztürk, N.; Akgöl, V.; Denizli, A. *Mater. Sci. Eng., C* **2009**, *29*, 2072–2078.
(26) Liu, X.; Hu, Q.; Fang, Z.; Zhang, X.; Zhang, B. *Langmuir* **2009**, *25*, 3–8.
(27) Huang, S.; Chen, D. *J. Hazard. Mater.* **2009**, *163*, 174–179.
(28) Saeed, K.; Haidera, S.; Oh, T. J.; Park, S. Y. *J. Membr. Sci.* **2008**, *322*, 400–405.
(29) Sutasinpromprae, J.; Jitjaicham, S.; Nithitanakul, M.; Meechaisue, C.; Supaphol, P. *Polym. Int.* **2006**, *55*, 825–833.
(30) Reneker, D. H.; Yarin, A. L. *Polymer* **2008**, *49*, 2387–2425.
(31) Shin, Y. M.; Hohman, M. M.; Brenner, M. P.; Rutledge, G. C. *Polymer* **2001**, *42*, 9955–9967.
(32) Ding, B.; Kim, H. Y.; Lee, S. C.; Shao, C. L.; Lee, D. R.; Park, S. J.; Kwag, G. B.; Choi, K. J. *J. Polym. Sci., Polym. Phys.* **2002**, *40*, 1261–1268.
(33) Wu, L. L.; Yuan, X. Y.; Sheng, J. *J. Membr. Sci.* **2005**, *250*, 167–173.
(34) Luu, Y. K.; Kim, K.; Hsiao, B. S.; Chu, B.; Hadjiargyrou, M. *J. Controlled Release* **2003**, *89*, 341–353.
(35) Kenawy, E. R.; Bowlin, G. L.; Mansfield, K.; Layman, J.; Simpson, D. G.; Sanders, E. H.; Wnek, G. E. *J. Controlled Release* **2002**, *81*, 57–64.
(36) Chen, C.; Lin, M.; Hsu, K. *J. Hazard. Mater.* **2008**, *152*, 986–993.
(37) Kyzas, G. Z.; Kostoglou, M.; Lazaridis, N. K. *Chem. Eng. J.* **2009**, *152*, 440–448.
(38) Jing, X.; Liu, F.; Yang, X.; Ling, P.; Li, L.; Long, C.; Li, A. *J. Hazard. Mater.* **2009**, *167*, 589–596.
(39) Kara, A.; Uzun, L.; Beşirli, N.; Denizli, A. *J. Hazard. Mater.* **2004**, *106B*, 93–99.
(40) Dinu, M. V.; Dragan, E. S. *React. Funct. Polym.* **2008**, *68*, 1346–1354.
(41) Monier, M.; Ayad, D. M.; Sarhan, A. A. *J. Hazard. Mater.* **2009**, *176*, 348–355.

AM1008024